

2500 Years of European Climate Variability and Human Susceptibility

Ulf Büntgen,^{1,2*} Willy Tegel,³ Kurt Nicolussi,⁴ Michael McCormick,⁵ David Frank,^{1,2} Valerie Trouet,^{1,6} Jed O. Kaplan,⁷ Franz Herzig,⁸ Karl-Uwe Heussner,⁹ Heinz Wanner,² Jürg Luterbacher,¹⁰ Jan Esper¹¹

¹Swiss Federal Research Institute for Forest, Snow and Landscape Research (WSL), 8903 Birmensdorf, Switzerland. ²Oeschger Centre for Climate Change Research, University of Bern, 3012 Bern, Switzerland. ³Institute for Forest Growth, University of Freiburg, 79085 Freiburg, Germany. ⁴Institute of Geography, University of Innsbruck, 6020 Innsbruck, Austria. ⁵Department of History, Harvard University, Cambridge, MA 02138, USA. ⁶Laboratory of Tree-Ring Research, University of Arizona, Tucson, AZ 85721, USA. ⁷Environmental Engineering Institute, École Polytechnique Fédérale de Lausanne, 1015 Lausanne, Switzerland. ⁸Bavarian State Department for Cultural Heritage, 86672 Thierhaupten, Germany. ⁹German Archaeological Institute, 14195 Berlin, Germany. ¹⁰Department of Geography, Justus Liebig University, 35390 Giessen, Germany. ¹¹Department of Geography, Johannes Gutenberg University, 55128 Mainz, Germany.

*To whom correspondence should be addressed. E-mail: buentgen@wsl.ch

Climate variations have influenced the agricultural productivity, health risk and conflict level of preindustrial societies. Discrimination between environmental and anthropogenic impacts on past civilizations, however, remains difficult because of the paucity of high-resolution palaeoclimatic evidence. Here we present tree ring-based reconstructions of Central European summer precipitation and temperature variability over the past 2500 years. Recent warming is unprecedented, but modern hydroclimatic variations may have at times exceeded in magnitude and duration. Wet and warm summers occurred during periods of Roman and Medieval prosperity. Increased climate variability from ~AD 250-600 coincided with the demise of the Western Roman Empire and the turmoil of the Migration Period. Historical circumstances may challenge recent political and fiscal reluctance to mitigate projected climate change.

Continuing global warming and potential associated threats to ecosystems and human health present a significant challenge to modern civilizations that already experience many direct and indirect impacts of anthropogenic climate change (1–4). The rise and fall of past civilizations have been associated with environmental change, mainly due to effects on water supply and agricultural productivity (5–9), human health (10) and civil conflict (11). Although many lines of evidence now point to climate forcing as one agent of distinct episodes of societal crisis, linking environmental variability to human history is still limited by the dearth of high-resolution palaeoclimatic data prior to the last millennium (12).

Archaeologists have developed oak (*Quercus spp.*) ring width chronologies from Central Europe (CE) that cover nearly the entire Holocene and have used them for the purpose of dating archaeological artefacts, historical buildings, antique artwork and furniture (13). The number of

samples contributing to these records fluctuates between hundreds and thousands in periods of societal prosperity, but decreases during phases of socio-economic instability (14). Chronologies of living (15) and relict oaks (16, 17) may reflect distinct patterns of summer precipitation and drought if site ecology and local climatology imply moisture deficits during the vegetation period. Annually resolved climate reconstructions that contain long-term trends and extend prior to Medieval times, however, depend not only on the inclusion of numerous ancient tree-ring samples of sufficient climate sensitivity, but also on frequency preservation, proxy calibration and uncertainty estimation (18–20).

In order to understand inter-annual to multi-centennial changes in CE April-June (AMJ) precipitation over the late Holocene, we used 7284 precipitation-sensitive oak ring width series from sub-fossil, archaeological, historical and recent material representing temperate forests in Northeast France (NEF), Northeast Germany (NEG) and Southeast Germany (SEG) (Fig. 1). Mean annual replication is 286 series with a maximum of 550 series during Roman times and lowest samples size of 44 series ~AD 400. Growth variations amongst the three regions are significantly ($p < 0.001$) correlated over the past two millennia: NEF/SEG at 0.53, SEG/NEG at 0.47 and NEF/NEG at 0.37 (SOM). Correlation coefficients between AMJ precipitation readings from three stations in NEF, NEG and SEG average at 0.31 over the common instrumental period (1921–1988), whereas the three regional oak chronologies correlated at 0.37 over the same interval (see Supporting Online Material (SOM) for details).

The temporal distribution of historical tree harvest (i.e., felling dates) mimics preindustrial deforestation and population trends (Fig. 2), implying substantial anthropogenic landscape perturbation over the last 2500 years (21). Increased felling dates reflect construction activity during the Late Iron Age and Roman Empire (~300 BC to AD 200) and

indicate the maximum expansion and deforestation of the Western Roman Empire (WRE) to have occurred ~AD 250. Reduced tree harvesting ~AD 250-400 coincides with the biggest CE historical crisis, the Migration Period (MP), a time marked by lasting political turmoil, cultural change and socio-economic instability (22, 23). Increasing timber harvest for construction is represented by abundant felling parallel to socio-economic consolidation from the 6th to the 9th centuries. Many earlier structures were replaced during a settlement boom in the 13th century (22, 23), eliminating much construction evidence from the central-medieval period (AD 900-1100). Construction activity during the last millennium was disrupted by the Great Famine and Black Death (19), as well as by the Thirty Years' War.

To assess climatic drivers of oak growth during industrial and preindustrial times, we compared chronologies of high-frequency variability with instrumental records, independent climate reconstructions and historical archives (SOM). A total of 87 different medieval written sources comprise 88 eyewitness accounts of regional hydroclimatic conditions (with 1-7 reports per year) resolved to the year or better, which corroborate 30 out of 32 of the extremes preserved in our oak record between AD 1013 and 1504, whereas 16 reports have been found to be contradictory (Fig. 3A). These observations further confirm the spatial signature of the climatic signal reflected by the oak network. Scaled precipitation anomaly composites calculated for the 12 most positive and the 16 most negative oak extremes back to AD 1500 reveal significant wet and dry CE summers, respectively (Fig. 3B; SOM). Independently derived extremes in pan-European oak growth over the last millennium match five out of eleven extremes at the CE network-level, and 21 out of 53 at the regional-scale (fig. S6).

The regional oak chronologies correlate on average at 0.39 with AMJ precipitation variability (1901-1980) averaged over 45-50°N and 8-10°E. Increased proxy/target coherency is obtained from the combined CE oak record, which correlates at 0.50-0.59 with inter-annual to multi-decadal variations in AMJ precipitation (fig. S9). Correlation between this study and an independent summer drought reconstruction from Central Germany (19) is 0.56 over the common AD 996-2005 period (Fig. 4). To complement our hydroclimatic reconstruction, we also developed a CE summer temperature proxy based on 1089 Stone pine (*Pinus cembra*) and 457 European larch (*Larix decidua*) ring width series from high-elevation sites in the Austrian Alps and adjacent areas (SOM). This composite record includes living trees, historical timber and sub-fossil wood, and correlates at 0.72-0.92 with inter-annual to multi-decadal variations in instrumental June-August (JJA) temperature (1864-2003). The new proxy is significantly positive correlated with 20th century JJA temperatures of CE and the Mediterranean region (SOM), and

possesses high- to low-frequency agreement with an independent maximum latewood density-based temperature surrogate from the Swiss Alps (18) ($r=0.35-0.44$; AD 755-2003) (Fig. 4).

AMJ precipitation was generally above average and fluctuated within fairly narrow margins from the Late Iron Age through most of the Roman Period until ~AD 250, whereas two depressions in JJA temperature coincided with the Celtic Expansion ~350 BC and the Roman Conquest ~50 BC. Exceptional climate variability is reconstructed for AD ~250-550, and coincides with some of the most severe challenges in Europe's political, social and economic history, the MP. Distinct drying in the 3rd century paralleled a period of serious crisis in the WRE marked by barbarian invasion, political turmoil and economic dislocation in several provinces of Gaul, including Belgica, Germania superior and Rhaetia (23, 24). Precipitation increased during the recovery of the WRE in the 300s under the dynasties of Constantine and Valentinian, while temperatures were below average. Precipitation surpassed early imperial levels during the demise of the WRE in the 5th century before dropping sharply in the first half of the 6th century. At the same time, falling lake levels in Europe and Africa (1, 25) accompanied hemispheric-scale cooling that has been linked with an explosive, near equatorial volcanic eruption in AD 536 (26), followed by the first pandemic of Justinian plague that spread from the Eastern Mediterranean in AD 542/543 (27). Rapid climate changes together with frequent epidemics had the overall capacity to disrupt the food production of agrarian societies (5-8). Most of the oak samples from this period originate from archaeological excavations of water wells and sub-fossil remains currently located in floodplains and wetlands (Fig. 2D), possibly attesting drier conditions during their colonization.

AMJ precipitation and JJA temperature began to increase from the end of the 6th century and reached climate conditions comparable to those of the Roman period in the early 800s. The onset of wetter and warmer summers is contemporaneous with the societal consolidation of new kingdoms that developed in the former WRE (22). Reduced climate variability from ~AD 700-1000, relative to its surroundings, matches the new and sustained demographic growth in the northwest European countryside, and even the establishment of Norse colonies in the cold environments of Iceland and Greenland (9). Humid and mild summers paralleled the rapid cultural and political growth of medieval Europe under the Merovingian and Carolingian dynasties and their successors (22). Average precipitation and temperature showed fewer fluctuations during the ~AD 1000-1200 period of peak medieval demographic and economic growth (21, 22). Wetter summers during the 13th and 14th centuries and a first cold spell ~1300 agree with the globally observed onset

of the Little Ice Age (20, 28), likely contributing to widespread famine across CE. Unfavorable climate may have even played a role in debilitating the underlying health conditions that contributed to the devastating economic crisis that arose from the second plague pandemic, the Black Death, which reduced the CE population after AD 1347 by 40-60% (19, 21, 27). The period is also associated with a temperature decline in the North Atlantic and the abrupt desertion of former Greenland settlements (9). Temperature minima in the early 17th and 19th centuries accompanied sustained settlement abandonment during the Thirty Years' War and the modern migrations from Europe to America.

The rate of natural precipitation and temperature change during the MP may represent a natural analog to rates of projected anthropogenic climate change. Although modern populations are potentially less vulnerable to climatic fluctuations than past societies have been, they also are certainly not immune to the predicted temperature and precipitation changes, especially considering that migration to more favorable habitats (21) as an adaptive response will not be an option in an increasingly crowded world (6). Comparison of climate variability and human history, however, prohibits any simple causal determination and other contributing factors, such as socio-cultural stressors must be considered in this complex interplay (7, 29). Nevertheless, the new climate evidence sets a palaeoclimatic benchmark in terms of temporal resolution, sample replication and record length. Our data provide independent evidence that agrarian wealth and overall economic growth might be related to climate change on high- to mid-frequency (inter-annual to decadal) time-scales. Preindustrial societies were sensitive to famine, disease and war, which were often driven by drought, flood, frost or fire events, as independently described by documentary archives (29). It also appears to be likely that societies can better compensate for abrupt (annual) climatic extremes and have the capacity to adapt to slower (multi-decadal to centennial) environmental changes (6, 7). Linking palaeo-demographic to climate proxy data challenges recent political and fiscal reluctance to mitigate projected global climate change (30), which reflects the common societal belief that civilizations are insulated from variations in the natural environment. The historical association between European precipitation and temperature variation, population migration and settlement desertion, however, questions the wisdom of this attitude.

References and Notes

1. T. M. Shanahan *et al.*, *Science* **324**, 377 (2009).
2. E. R. Cook, R. Seager, M. A. Cane, D. W. Stahle, *Earth Sci. Rev.* **81**, 93 (2007).
3. M. E. Mann, J. D. Woodruff, J. P. Donnelly, Z. Zhang, *Nature* **460**, 880 (2009).
4. E. R. Cook *et al.*, *Science* **328**, 486 (2010).

5. B. M. Buckley *et al.*, *Proc. Natl. Acad. Sci. U.S.A.* **107**, 6748 (2010).
6. H. Weiss, R. S. Bradley, *Science* **291**, 609 (2001).
7. P. B. deMenocal, *Science* **292**, 667 (2001).
8. G. H. Haug *et al.*, *Science* **299**, 1731 (2003).
9. W. P. Patterson, K. A. Dietrich, C. Holmden, J. T. Andrews, *Proc. Natl. Acad. Sci. U.S.A.* **107**, 5306 (2010).
10. A. J. McMichael, R. E. Woodruff, S. Hales, *Lancet* **367**, 859 (2006).
11. M. B. Burke, E. Miguel, S. Satyanath, J. A. Dykema, D. B. Lobell, *Proc. Natl. Acad. Sci. U.S.A.* **106**, 20670 (2009).
12. P. D. Jones *et al.*, *Holocene* **19**, 3 (2009).
13. K. Haneca, K. Čufar, H. Beeckman, *J. Archaeol. Sci.* **36**, 1 (2009).
14. W. Tegel, J. Vanmoerkerke, U. Büntgen, *Quat. Sci. Rev.* **29**, 1957 (2010).
15. D. A. Friedrichs *et al.*, *Tree Physiol.* **29**, 39 (2009).
16. P. M. Kelly, H. H. Leuschner, K. R. Briffa, I. C. Harris, *Holocene* **12**, 689 (2002).
17. K. Čufar, M. De Luis, D. Eckstein, L. Kajfez-Bogataj, *Int. J. Biometeorol.* **52**, 607 (2008).
18. U. Büntgen, D. C. Frank, D. Nievergelt, J. Esper, *J. Clim.* **19**, 5606 (2006).
19. U. Büntgen *et al.*, *Quat. Sci. Rev.* **29**, 1005 (2010).
20. D. C. Frank *et al.*, *Nature* **463**, 527 (2010).
21. J. O. Kaplan, K. M. Krumhardt, N. Zimmermann, *Quat. Sci. Rev.* **28**, 3016 (2009).
22. M. McCormick, *Origins of the European Economy. Communications and Commerce, A.D. 300-900* (Cambridge Univ. Press, Cambridge, 2001).
23. R. Duncan-Jones, in *Approaching Late Antiquity. The Transformation from Early to Late Empire*, S. Swain, M. Edwards, Eds. (Oxford Univ. Press, Oxford, 2004).
24. C. Witschel, *J. Roman Archaeol.* **17**, 251 (2004).
25. D. J. Charman, A. Blundell, R. C. Chiverrell, D. Hendon, P. G. Langdon, *Quat. Sci. Rev.* **25**, 336 (2006).
26. L. B. Larsen *et al.*, *Geophys. Res. Lett.* **35**, L04708 (2008).
27. K. L. Kausrud *et al.*, *BMC Biol.* **8**, 112 (2010).
28. V. Trouet *et al.*, *Science* **324**, 78 (2009).
29. R. Brázdil, C. Pfister, H. Wanner, H. von Storch, J. Luterbacher, *Clim. Change* **70**, 363 (2005).
30. D. B. Lobell *et al.*, *Science* **319**, 607 (2008).
31. We thank E. Cook, G. Haug, D. Johnson, N. Stenseth, E. Zorita and two anonymous referees for comments and discussion. The authors acknowledge supported by the SNSF (NCCR-Climat), the DFG (PRIME, INTERDYNAMIK, Historical Climatology of the Middle East based on Arabic sources back to AD 800), the FWF (P15828, F3113-G02), the INRAP, the Andrew W. Mellon

Foundation, as well as the EU projects Millennium (017008) and ACQWA (212250).

Supporting Online Material

www.sciencemag.org/cgi/content/full/science.1197175/DC1

Materials and Methods

Figs. S1 to S12

Tables S1 and S2

References

31 August 2010; accepted 5 January 2011

Published online 13 January 2011; 10.1126/science.1197175

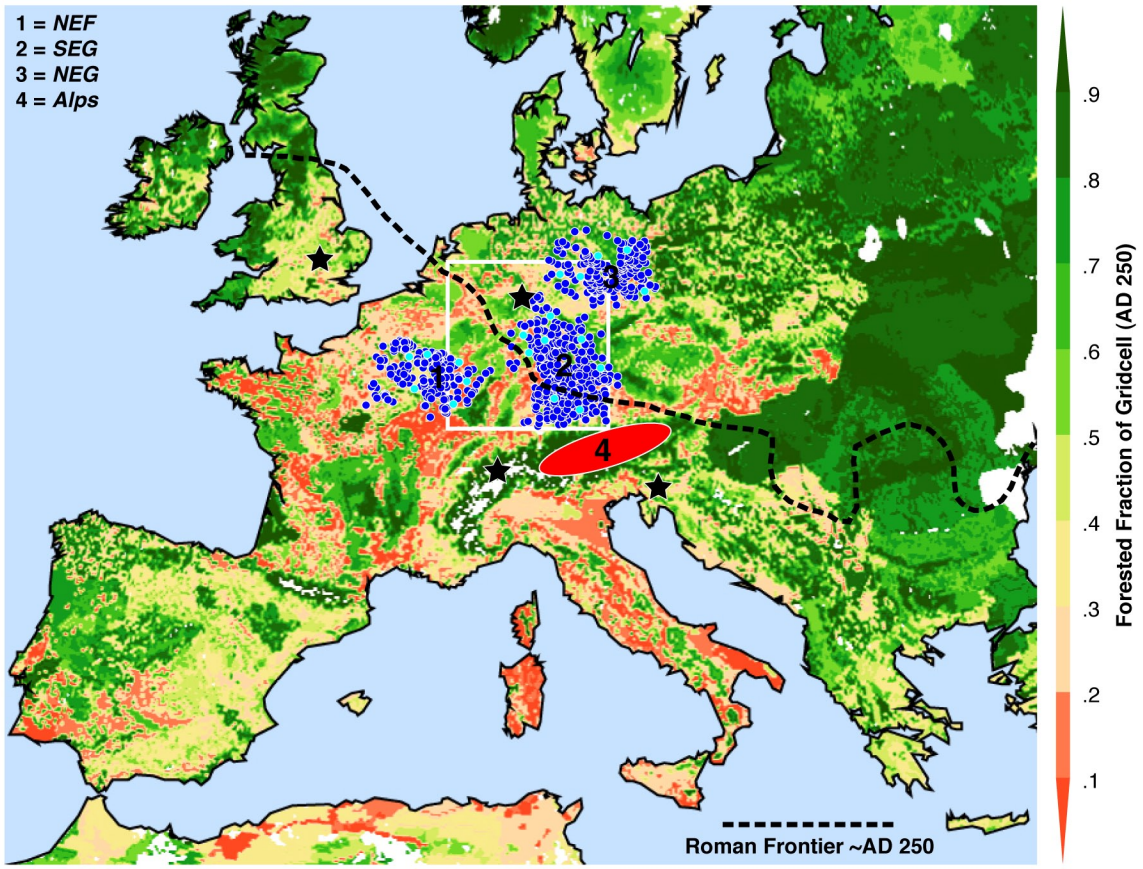
Fig. 1. Location of the 7284 CE oak samples (blue) and the network of 1546 Alpine conifers (red), superimposed on a deforestation model of Roman land-use/land-cover ~AD 250 (20). Black stars indicate the location of the independent tree-ring chronologies used for comparison (16–19), and the white box refers to the area over which gridded precipitation totals were averaged and used for proxy calibration.

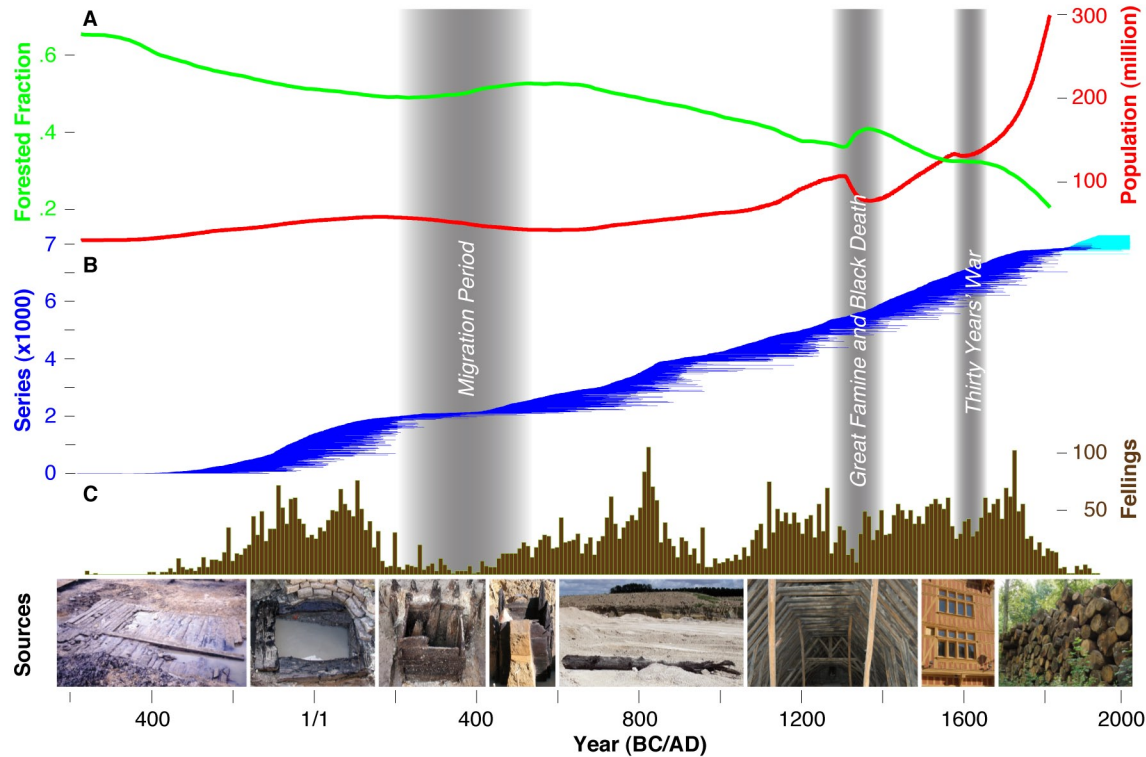
Fig. 2. (A) Evolution of CE forest cover and population, together with (B) oak sample replication, (C) their historical end-dates at decadal-resolution, and (D) examples of archaeological (Left), sub-fossil, historical and recent (Right) sample sources.

Fig. 3. (A) Correlation map of the mean oak chronology against gridded CE AMJ precipitation data (1901–1980) together with the location of 104 historical reports of which 88 witnesses corroborate 30 out of 32 climatic extremes that were reconstructed from the oak data between 1013 and 1504, whereas 16 witnesses offer contradictory reports. Note that different reports may originate from the same location. (B) Composite anomaly fields (scaled means, modified *t*-values) of summer (JJA) precipitation computed for 12 positive (Top) and 16 negative (Bottom) oak extremes between 1500 and 2000 (SOM). Significance of the composite anomalies, relative to the 1901–2000 climatology, was computed using 95% confidence thresholds of the modified two-sided *t* test (SOM). Blue and red colors refer to significant wet and dry conditions, respectively. Green dots refer to the location of 7284 CE oak samples.

Fig. 4. Reconstructed AMJ precipitation totals (Top) and JJA temperature anomalies (Bottom) (wrt 1901–2000). Error bars are ± 1 RMSE of the calibration periods. Black lines show independent precipitation and temperature reconstructions from Germany (19) and Switzerland (18). Bold lines are 60-year low-pass filters. Periods of demographic expansion, economic prosperity and societal stability, as well as political turmoil, cultural change and population instability are marked (green and grey text).

- 1 = NEF
- 2 = SEG
- 3 = NEG
- 4 = Alps





Spatial Field Correlation & Historical Agreement

